Trends in Strong Chemical Bonding in C2, CN, CN-, CO, N2, NO, NO+, and O2

Kepp, Kasper Planeta

Published in:
Journal of Physical Chemistry Part A: Molecules, Spectroscopy, Kinetics, Environment and General Theory

Link to article, DOI:
10.1021/acs.jpca.7b08201

Publication date:
2017

Document Version
Peer reviewed version

Trends in Strong Chemical Bonding in C_2, CN, CN^-, CO, N_2, NO, NO^+, and O_2

Kasper P. Kepp*

Technical University of Denmark, DTU Chemistry, Building 206, 2800 Kgs. Lyngby, DK – Denmark. *Phone: +045 45 25 24 09. E-mail: kpj@kemi.dtu.dk

ABSTRACT: The strong chemical bonds between C, N, and O play a central role in chemistry, and their formation and cleavage are critical steps in very many catalytic processes. The close-lying molecular orbital energies and large correlation effects pose a challenge to electronic structure calculations and have led to different bonding interpretations, most notably for C_2. One way to approach this problem is by strict benchmark comparison of related systems. This work reports reference electronic structures and computed bond dissociation enthalpies D_0 for C_2, CN, CN^-, CO, N_2, NO, NO^+, O_2 and related systems C_2^+ and C_2^- at chemical accuracy (~1 kcal/mol or 4 kJ/mol) using CCSD(T)/aug-cc-pV5Z, with additional benchmarks of HF, MP2, CCSD, explicitly correlated F12 methods, and four density functionals. Very large correlation and basis set effects are responsible for up to 93% of total D_0. The order of the molecular orbitals $1\pi_u$ and $3\sigma_g$ changes, as seen in text books, depending on total and effective nuclear charge. Linear trends are observed in $2\sigma_u - 2\sigma_g$ orbital splitting ($R^2 = 0.91$) and in D_0 of C_2, C_2^-, and C_2^+ ($R^2 = 0.99$). The correlation component of D_0 of C_2 is by far the largest (~93%) due to a poor HF description. Importantly, density functional theory fails massively in describing this series consistently in both limits of effective nuclear charge, and Hartree-Fock exchange or meta functionals do not remedy this 100 kJ/mol-error, which should thus be addressed in future density functional developments as it affects very many studies involving cleavage or formation of these bonds.

INTRODUCTION

The diatomic molecules of second-period elements C, N, and O are fundamental to our understanding of chemistry and are the basis of teaching chemical bonding and molecular orbital (MO) theory in chemistry classes[1–3]. N_2 is notoriously inert and present at 78% in the atmosphere, whereas O_2, with its paramagnetic state and role as main electron acceptor of higher life forms, makes up most of the remaining part. CO and NO are important biological messenger molecules[4,5] and are central to a wide range of catalytic processes[6], and the molecules play a major role as ligands in coordination chemistry[7–9].

Accordingly, these simple molecules have been widely studied for a long time[1,2,10,11]. N_2 has revealed the dramatic failure of Møller-Plesset perturbation theory for such systems[12], which require accurate treatment of electron correlation[13,14]. The $1\pi_u$ and $3\sigma_g$ molecular orbitals are conspicuously close in energy and differ in their occupation as noted in typical text books[3]. As discussed further below, even the $2\sigma_u$ MO can be close to $1\pi_u$ and $3\sigma_g$, providing in some cases space for eight electrons within 0.2-0.3 eV. Some of the strongest bonds known in chemistry include the triple bonds of CN^-, CO, and N_2. The molecules routinely enter density functional calculations via the description of catalytic processes, even though these tightly bound systems can produce large errors that could affect overall reliability of such studies. As an example, any model that estimates how O_2 or N_2 is cleaved by a catalyst is sensitive to the chosen method's error in describing the respective bond dissociation enthalpy, D_0[15,16].

Because of this complexity, our understanding of the chemical bonding in these species is regularly challenged, both during interaction with transition metal complexes such as O_2 binding to heme[17–20], and for the bonds themselves, as is the case for C_2[21–26]. In both examples, the different

interpretations from MO theory and valence bond theory play a notable role: Thus, C_2 can yield valence bond structures resembling a quadruple bond[24,27,28]. Single-determinant MO theory traditionally describes C_2 as a double bond[22,25,29,30], but different orbital definitions in the configuration state functions from multi-configurational self-consistent field (MC-SCF) methods can help reconcile MO and valence bond theory[31,32]. The main requirement of any such model is of course 1) agreement with all available experimental data, notably D_0, and 2) predictive value, e.g. in relation to catalytic cleavage of the chemical bond in question.

Particular questions of interest include: 1) What is required to accurately (within 1 kcal/mol) compute D_0 of these molecules? 2) How large are the correlation effects in these strongly bonded molecules? 3) What is the order of MO energies in the various species and how does it affect bonding? 4) To which extent do density functionals have problems with these systems? 5) Do any of the molecules behave irregularly in the overall comparison, and if so, how? To address these questions, the electronic structures of a range of diatomic molecules and molecular ions were computed with the aim to reproduce experimental D_0 to within chemical accuracy (defined as errors smaller than 1 kcal/mol or ~4 kJ/mol) and subsequently, at this level of accuracy, analyze trends in electronic structure.

COMPUTATIONAL DETAILS

All computations were performed using the Turbomole software, version 7.0[33]. All densities and energies were converged to 10^{-7} a.u., and the resolution of identify approximation was used to speed up all HF, MP2, CCSD, and CCSD(T) calculations[34,35]. In some cases also the explicitly correlated F12-CCSD and F12-CCSD(T) results were computed[36]. Experimental bond lengths from NIST were used as follows: NO^+ = 1.0657 Å, NO = 1.1538 Å, O_2 = 1.2075 Å, N_2 = 1.0977

Å, CO = 1.1282 Å, CN = 1.1718 Å, CC = 1.2425 Å; CN^- = 1.177 Å. The energies of all molecules and atoms were computed using the aug-cc-pV5Z basis set[37] (numerical data in Table S1 with errors vs. experiment in Table S2). The bond dissociation enthalpies were computed as:

$$D_0\,(XY) = E_{el}\,(X) + E_{el}\,(Y) - E_{el}\,(XY) - ZPE\,(XY) \qquad (1)$$

where $E_{el}\,(X)$ is the electronic energy of species X computed and ZPE(XY) is the vibrational zero-point energy of XY (numerical details in Table S3). For NO^+, the fragments are N and O^+, because any double occupation of p-orbitals is avoided, as seen also by comparison of the energies E(N) + $E(O^+)$ vs. $E(N^+)$ + E(O) (Supporting Information, Table S1). Similar reasoning applies to CN^-, which forms C^- and N[38]. To investigate the role of the basis set in describing accurately the bonding, the following smaller basis sets were further tested for all eight molecules C_2, CN, CN^-, CO, N_2, NO, NO^+, and O_2: def2-SVP, def2-TZVPP, def2-QZVPP[39], aug-cc-pVTZ, and aug-cc-pVQZ[37] (numerical data in Tables S4-S10). Scalar-relativistic corrections (Cowan-Griffin approximation[40]) for the energies of X , Y and XY were also computed and increase the D_0 by 0.3-1.3 kJ/mol, the least for C_2 and the most for NO^+, in line with the effective nuclear charge and associated compactness of the 1s orbitals (Table S11). Hence, relativistic corrections were not considered further in this work. As the experimental data are in gas phase, the enthalpy corrections $\Delta H(X)$ were further computed as 3/2 RT for each D_0.

Four density functionals were investigated to understand how such methods perform in the "tight-bonding" regime studied here: PBE0, PBE, B3LYP, and TPSSh. Among these, PBE0[41] and B3LYP[42–44] represent hybrid GGA functionals with 25% and 20% HF exchange, whereas PBE is a GGA non-hybrid[41], and TPSSh is a meta hybrid functional[45,46]. To understand C_2 in more detail, C_2^+, C_2^-, C^+, and C^- were also studied as specified in Table S12, in order to compute D_0 of C_2^+ and C_2^- for comparison with C_2 (numerical details in Table S13). The geometries of C_2^+, and C_2^- were

obtained by geometry optimization at the B3LYP/def2-TZVPP level, which gives an error vs. the experimental bond lengths of C_2 of 0.005 Å (B3LYP: 1.247 Å; BLYP: 1.256 Å; TPSSh: 1.251 Å).

RESULTS AND DISCUSSION

Correlation and Basis Set Effects on Computed D_0 Values. The D_0 values were computed according to Equation (1), using HF, MP2, CCSD, CCSD(T), and the four density functionals PBE0, PBE, TPSSh, and B3LYP, and are shown in Table 1. The computed zero-point energies of the molecules (Table S3 in Supporting Information) range from 10-15 kJ/mol (9.7 for O_2; 14.6 for NO^+) and are thus required to accurately reproduce the experimental D_0. In contrast, relativistic corrections affect D_0 by ~1 kJ/mol for the systems (Supporting Information, Table S11) and thus do not affect accuracy, as expected for second-period atoms.

Table 1. Computed D_0 (kJ/mol) using different methods corrected for zero-point energy and enthalpy (+3/2 RT); basis set: aug-cc-pV5Z.

	HF	MP2	CCSD	CCSD(T)	PBE0	PBE	TPSSh	B3LYP	EXP.	E_{corr}[a]
NO^+	502.0	1105.7	1000.2	1046.1	1048.2	1150.8	1042.1	1063.8	1046.9	0.52
O_2	134.0	545.7	461.9	497.0	516.5	595.5	497.7	509.0	498.5	0.73
NO	215.7	659.4	589.3	627.9	635.7	712.6	619.7	637.4	630.6	0.66
N_2	472.5	995.6	902.2	942.4	934.2	1008.6	917.2	944.9	944.9	0.50
CO	721.0	1136.4	1045.1	1079.0	1060.9	1115.4	1035.9	1055.3	1076.6	0.33
CN	369.6	697.6	701.6	742.7	740.4	816.8	729.3	737.8	749.3	0.50
CC	42.9	658.0	525.0	608.5	497.4	594.3	495.1	489.2	605.0	0.93
CN^-	604.0	1050.3	964.9	1000.7	978.2	1025.3	958.7	993.7	N/A	0.40
MSE	***-442.0***	***35.2***	***-46.6***	***-1.2***	***-16.9***	***64.4***	***-29.4***	***-15.1***		
MAE	***442.0***	***50.0***	***46.6***	***2.8***	***23.9***	***67.1***	***29.6***	***26.3***		

[a] Correlation energy contribution to D_0, estimated as D_0(CCSD(T) – D_0(HF) / D_0(CCSD(T).

Table 1 shows that CCSD(T)/aug-cc-pV5Z achieves chemical accuracy (MAE ~2.8 kJ/mol) for these systems. Thus, CCSD(T) at this basis set level accurately describes the bonding and correlation energy of the systems. From Table 1, the correlation energy, defined as $E_{CCSD(T)} - E_{HF}$, constitutes a very large part and often more than half of the total D_0. C_2 stands out by having a very poor HF description of bonding, as pointed out previously[3], and a corresponding very large (~ 93%) contribution of correlation energy to D_0. This makes the C-C bond in C_2 the most correlated of those in the series.

Table 2. D_0 computed for C_2 using different wave-function methods and basis sets.

Basis set	HF	MP2	CCSD	CCSD(T)	F12-CCSD	F12-CCSD(T)
aug-cc-pV5Z	41.7	656.7	523.8	607.2	523.9	606.1
aug-cc-pVQZ	41.6	650.2	519.2	601.4	524.6	604.7
aug-cc-pVTZ	39.0	648.6	522.7	601.9	525.8	601.2
def2-QZVPP	41.5	647.0	517.1	598.8	525.9	604.9
def2-TZVPP	40.2	628.0	502.6	580.9	524.9	598.8
def2-SVP	40.7	612.1	513.0	585.1	552.9	616.7

As seen from a basis set effect study of C_2 in Table 2, high accuracy is only achieved when using very large basis sets, and chemical accuracy (1 kcal/mol) requires aug-cc-pV5Z. Basis set effects have been studied before for some of these molecules, reaching similar conclusions[12,47]. Even a polarized triple-zeta basis set underestimates bonding considerably. This can be traced to the large correlation energy and substantial electron-electron cusp of the tightly bound electrons as previously discussed for N_2[48]. Basis set effects for the other seven molecules are summarized in Supporting Information, Tables S4-S10. The basis set effects estimated from CCSD(T) are larger for the triple-bonded N_2 (~77.8 kJ/mol from def2-SVP to aug-cc-pV5Z, Table S4). For O_2 the largest difference is 47.6 kJ/mol, whereas it is 58.5 kJ/mol for NO. The basis set errors for all eight molecules scale somewhat with D_0 (correlation coefficient of linear regression R ~ 0.33) as estimated by plotting the standard deviation of computed D_0 for the six basis sets against D_0 at the

CCSD(T)/aug-cc-pV5Z level (Figure S1). C_2 which has an average D_0 in the series thus has a less pronounced basis set effect of 22.1 kJ/mol (Table 2).

Although Table 1 already shows that the basis set is saturated from the point of view of D_0 at aug-cc-pV5Z (as seen from the uniform high accuracy for all systems), a further validation of the basis set saturation was carried out using explicitly correlated F12 methods[49] for CCSD, and CCSD(T)[36], as shown in the last two columns of Table 2; they show faster convergence with smaller basis sets towards the value of the aug-cc-pV5Z basis set. Chemical accuracy is achieved at the polarized quadruple-zeta or even triple-zeta level using F12 methods because the electron-electron cusp is recovered at lower basis set costs. Polarization functions are essential to polarize electrons within the bonding region. Again, MP2 consistently overbinds and CCSD consistently underbinds relative to CCSD(T) for a given basis set. Importantly, D_0 increases monotonically with basis set size, because the tightly bound diatomic molecules benefit the most from additional freedom to distribute the electrons. Since small basis sets underbind, MP2 provides an example of commonly encountered error cancellation, with MP2/def2-TZVPP being within 10 kJ/mol of experiment due to cancellation of errors in the one-electron basis and correlation treatment.

As seen from Table 2, any model based on a triple-zeta basis set or smaller will miss some part of D_0, as the electrons are not optimally distributed in the bonding region. An indication of this is seen in Supporting Information, Figure S2, showing that differences in the electron density along the bond axis are very basis-set dependent. More electron density is recruited to the bonding region as correlation is recovered accurately.

Trends in Accuracy vs. Effective Nuclear Charge. The individual errors for each method and system, defined as D_0 (computed) - D_0(experimental), are shown in Figure 1 (numerical data in Table S2). The largest error for CCSD(T) (6.6 kJ/mol) is seen for the open-shell molecule CN, and uniform high accuracy is otherwise evident. Figure 1 shows that both MP2 and CCSD fail in

producing accurate bonding, and they miss by approximately the same amount in most cases, but in different directions such that CCSD underbinds and MP2 overbinds; accordingly, $E = ½ (E_{MP2} + E_{CCSD})$ gives a conspicuously good estimate of D_0 in most cases (except for CN).

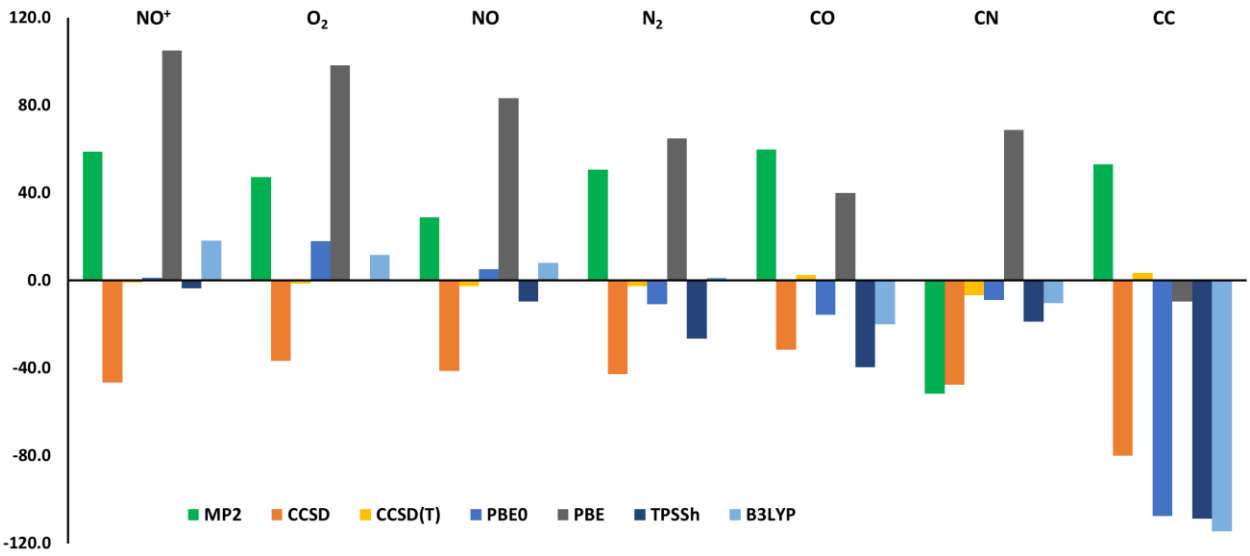

Figure 1. Errors in computed D_0, corrected for vibrational zero-point energies and enthalpy.

The molecules in Figure 1 have been ordered according to effective nuclear charge, with the highest effective nuclear charge listed to the left (this order is also the same as for the general trend in MO energies, as discussed below). From this choice of ordering, some interesting observations can be made: While the *ab initio* methods MP2, CCSD, and CCSD(T) show no general trend in D_0 (computed) - D_0(experimental) with this ordering, the density functionals all show a trend, in particular if CN is placed with the other open-shell molecule NO. For PBE, the trend is very clear because the GGA functional overbinds by > 100 kJ/mol for NO^+, with a trend towards good accuracy but somewhat underbinding in C_2. However, the three hybrid functionals confirm this tendency but are generally less strongly binding, and are thus accurate for NO^+, O_2, and NO, but increasingly inaccurate due to underbinding in N_2, CN, CO, and in particular C_2. C_2 stands notably out in the series with the smallest effective nuclear charge and the most diffuse

electrons; the hybrid functionals and CCSD fail to bind strongly enough and any hybrid functional, regardless of the amount of HF exchange, underbinds by 100 kJ/mol.

This comparison shows that none of the density functionals provide a balanced description of bonding through the series, and the imbalance amounts to ~100 kJ/mol for all four density functionals: *In other words, no density functional is capable of describing this series even remotely correctly in both limits of high and low effective nuclear charge*. Because the aug-cc-pV5Z basis set is saturated as shown above, this discrepancy is due to the functional design, but neither HF exchange at any amount, nor the meta functional character (TPSSh), nor the quantum mechanical bounds on the density imposed by PBE and TPSSh can remedy this error, which relates to the balance between tight and weak bonding regimes enforced by the effective nuclear charge. This makes the series studied here an outstanding problem to DFT that begs further scrutiny also in the development of new functionals. This is particularly true because of the importance of these molecules in catalysis, and because the 100-kJ/mol errors will strongly affect the reliability of DFT studies in catalysis where O-O, C-O, and N-O bonds are formed or cleaved.

Ordering of Molecular Orbital Energies. Figure 2 shows the HF molecular orbital energies of the largest basis set, aug-cc-pV5Z, ordered according to decreased effective nuclear charge. For the unrestricted calculations the energies are averages of the α- and β-orbitals. For smaller basis sets, the more diffuse virtual MOs would be less well described than occupied MOs but at this basis set level, the general trends are quite smooth and thus worthy of discussion. For the neutral species the $1\pi_u$ orbitals change regularly and only by about 0.2 eV due to effective nuclear charge from O_2, over NO, N_2, CO, and CN, to C_2, whereas all the σ-orbitals $2\sigma_g$, $2\sigma_u$ and $3\sigma_g$ change by ~0.5 eV along the neutral series, because their more compact nature renders them more sensitive to nuclear charge; this difference is responsible for the change in MO ordering. N_2 and O_2 have the same order of MOs, with $3\sigma_g$ slightly lower than $1\pi_u$, as confirmed also for the

intermediate case NO. However, in CO, more so in CN, and even more so in C_2 (in order of reduced effective nuclear charge) $3\sigma_g$ increases substantially in energy compared to $1\pi_u$ because $3\sigma_g$ (which is formed by the p_z orbitals) is more sensitive to the reduced effective nuclear charge than $1\pi_u$. In CN^- the total charge of an additional electron causes destabilization of all MOs, compared to CN.

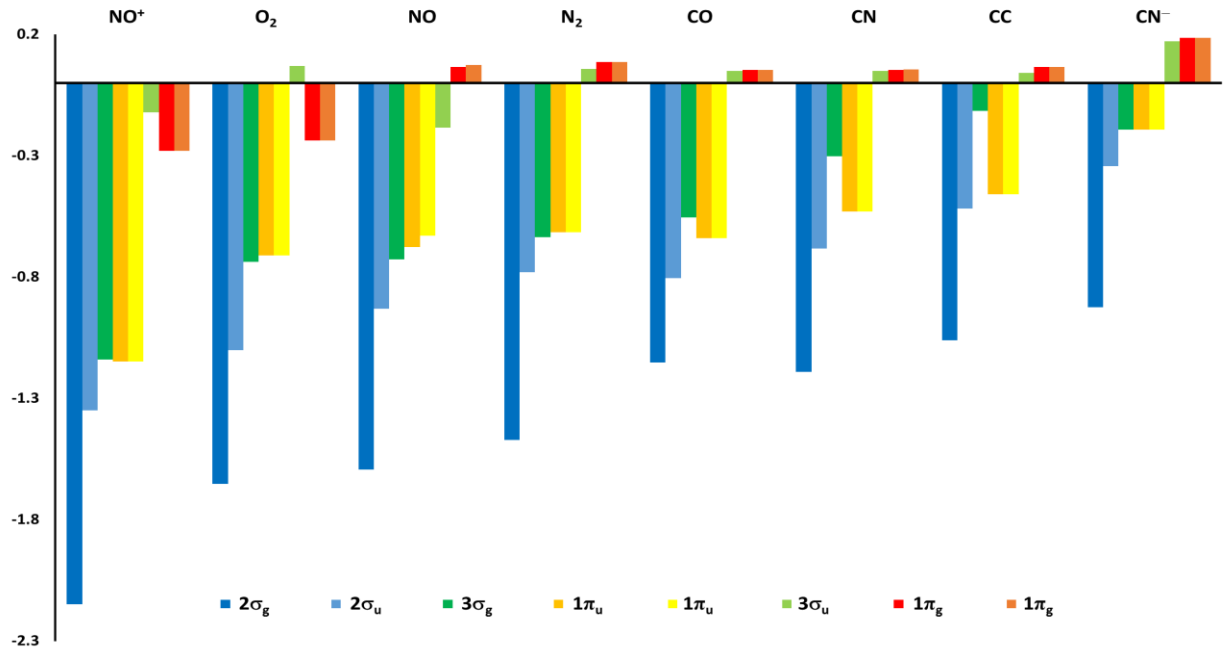

Figure 2. HF/aug-cc-pV5Z orbital energies (average of alpha and beta for unrestricted calculations).

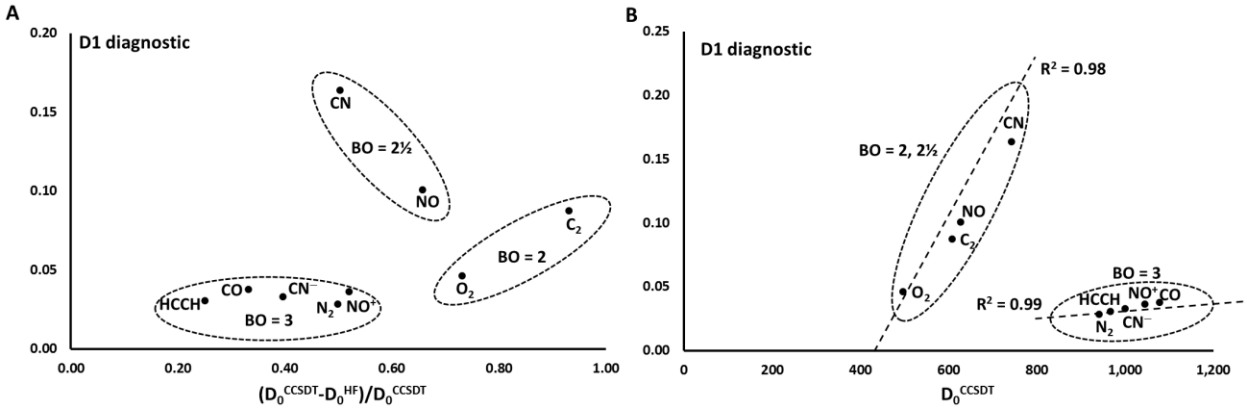

Figure 3. D1 diagnostic for the CCSD plotted against **A)** the fraction of the total bond dissociation enthalpy due to correlation, ($D_0^{CCSD(T)} - D_0^{HF}$) / $D_0^{CCSD(T)}$, **B)** total computed $D_0^{CCSD(T)}$.

Correlation Complexity (Measured by D1) Grows Linearly with Bond Strength. To further understand the challenge of describing the bonding in these molecules, Figure 3 shows the D1 diagnostic obtained for the CCSD calculations[50] at the aug-cc-pV5Z level, plotted against the fraction of D_0 that is due to correlation (Figure 3A) and the total D_0, computed at the CCSD(T) level (Figure 3B). The first plot indicates how the quality of the CCSD calculation depends on how important electron correlation is for the total bond energy, whereas the second plot simply shows the correlation with total D_0. Except for the radicals CN and NO, and C_2 all D1 diagnostics are smaller than 0.05, implying that CCSD treats these systems well without any complications of multi-configuration mixing. However, C_2 is notable by having the clearly largest D1 value among the closed-shell systems. The same order for three of these molecules CN > C_2 > O_2 was obtained previously[50]. All the triple-bonded closed-shell systems display low D1 values and also cluster tightly in the plot against the correlation component of D_0 (Figure 3A). For the two other groups of formal bond orders (BO) 2½ and 2, the molecule with the smallest effective nuclear charge displays the highest D1 diagnostic, consistent with the challenge of computational chemistry discussed above relating to the low effective nuclear charge. When D1 is plotted directly against D_0 as shown in Figure 3B, however, strongly linear relationships are obtained for the two groups of BO = 2, 2½, and BO = 3, showing that the quality of the CCSD treatment decreases essentially linearly (R^2 = 0.98-0.99) with the strength of bonding, i.e. the tight bonding regime, which again relates to the electron cusp as discussed previously for N_2[48], but the sensitivity is much larger for the BO = 2,2½ group where the open-shell molecules and extreme C_2 case occur.

Correlation Effects and Bonding in C_2. While the comparison above provides insight into the series of molecules as a whole, in the following the special case of C_2 is discussed a bit more due to its prominent featuring in recent discussions[22–25,27]. The most significant debate is on the suitability of describing C_2 as a quadruply bound molecule using valence bond theory or simply

as a double bond as obtained from MO diagrams. As discussed previously[24,27], valence bond theory can lead to construction of a fourth loose bond formed by the two anti-bonding (in MO theory) $2\sigma_u$ electrons, whereas in single-determinant MO theory this orbital is considered strictly anti-bonding. One argument against the double bonded C_2 is that $2\sigma_u$ is "fuzzy", i.e. it is only weakly anti-bonding or perhaps even non-bonding. In valence bond theory these two electrons can be described as being in an "inverted" bond[28].

Without going into discussions on this debate, it is relevant to discuss C_2 within the present benchmark CCSD(T)/aug-cc-pV5Z computations because they provide D_0 at chemical accuracy (Table 1) as not seen in these previous discussions on C_2. One way to do this is by bonding analysis, which has been done excessively in the past[24–27,29]. Another is to compare directly the electronic correlation energies at the CCSD(T)/aug-cc-pV5Z level, where experimental D_0 is recovered, for a series of related systems that includes C_2.

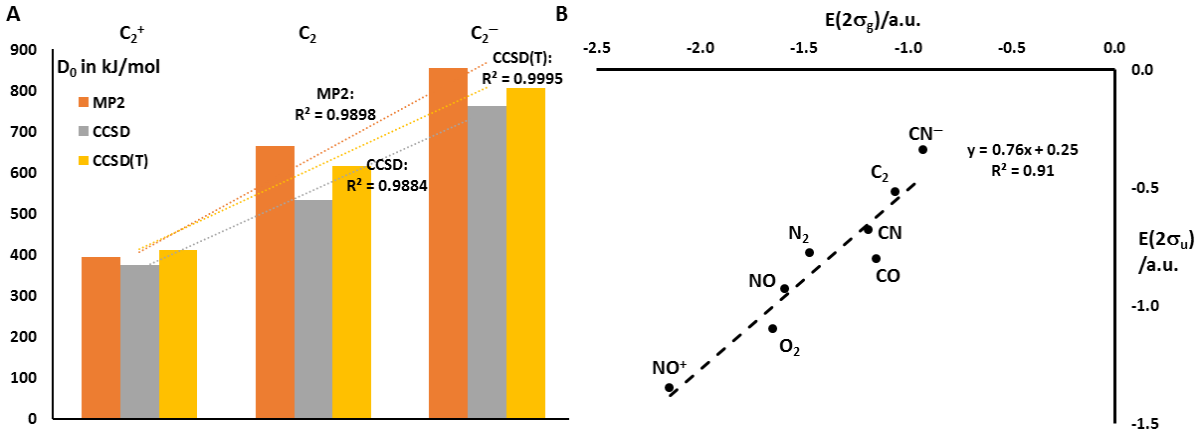

Figure 4. A) The trends in D_0 computed using MP2, CCSD, and CCSD(T) for C_2^+, C_2, and C_2^-; all three methods show almost perfectly linear trends in D_0. **B)** Plot of the energy of the bonding $2\sigma_g$ vs. that of the anti-bonding $2\sigma_u$ for NO^+, NO, O_2, N_2, CO, CN, C_2, and CN^-.

Figure 4A shows a comparison of D_0 obtained using MP2, CCSD, and CCSD(T) for C_2 and its one-electron-enriched or depleted counterparts, C_2^- and C_2^+ (numerical data in Tables S12 and S13). According to MO theory, the C_2 bond should be between C_2^- and C_2^+ in strength because the additional electron is placed in the $3\sigma_g$ orbital which is bonding, and formally the BO increases from 2 to 2½, whereas in C_2^+ a bonding electron is lost from $1\pi_u$ (see Figure 1) to produce a BO of 1½. It is not clear what the relationship will be if the true bonding in C_2 is distinct from what simple single-determinant MO theory predicts (BO = 2). Possibly D_0 of C_2 would still be smaller than D_0 of C_2^-, but if the bond in C_2 is unique, one would expect some deviation from an exact linear trend, if C_2^- and C_2^+ are normal and disrupt the unique quadruple bond character, even if C_2^- is stronger as measured by D_0. Figure 4A shows almost perfectly linear relationships for D_0 computed with *all* three methods MP2, CCSD, and CCSD(T) with R^2 values of 0.99, i.e. C_2 falls exactly in between C_2^- and C_2^+ in terms of its D_0. This observation is fully in agreement with the expectations from basic MO theory of a double bonded C_2, but it is possible that valence bond theory can also explain this linearity with C_2 still being qualitatively different from the two other bonds.

Figure 4B shows another comparison of the energies of the bonding $2\sigma_g$ vs. the energy of the anti-bonding $2\sigma_u$ for NO^+, NO, O_2, N_2, CO, CN, C_2, and CN^-. In single-determinant MO theory these two orbitals form a tightly correlated bonding-antibonding set, and the antibonding orbital $2\sigma_u$ plays a major role in the left-right electron correlation description of the bonds. Both these two orbitals become more negative with higher effective nuclear charge, as expected. The linear regression suggests that the two orbitals are strongly correlated with $R^2 = 0.91$ and C_2 falls very close to the regression line. These electrons are mainly located along the (left-right correlated) axis of the molecules and thus do not interfere with the π-system.

One picture that summarizes these various observations is that C_2 represents very strong left-right correlation due to the low effective nuclear charge combined with the tight bonding, an effect that forces electrons that are formally anti- or non-bonding into the bonding region and requires very large augmented basis sets (Table 2). Such strong left-right correlation in C_2, CN, and CN^- could be interpreted as additional bonding in various bonding models, yet it does not significantly affect D_0 which is perfectly normal, probably because this electron movement is compensated by alternative movements of other electrons as witnessed by the very large role of basis sets and triple corrections to CCSD. Thus, putting eight electrons in the bonding region is too costly even though it would complete the octet rule, but it takes a very large basis set and CCSD(T) to see the compensation that makes C_2 behave normally in Figure 4.

CONCLUSIONS

In summary, the experimental D_0 is well reproduced for all studied molecules where data are available using CCSD(T)/aug-cc-pV5Z; less correlated methods such as MP2 and CCSD are not sufficient, and smaller basis sets even at the quadruple-zeta level are not sufficient either. Thus, models based on limited basis sets may wrongly estimate D_0 and the amount of electrons formally residing in the bonding region. It is shown that electron correlation constitutes most of the bond energy in these tightly bound systems, and C_2 is extreme in this regard as the HF picture is very poor. The correlation energy amounts to an amazing 93% of the D_0 of C_2. Using the chemical accuracy CCSD(T) calculations, the D_0 of C_2 is shown to fall perfectly on a line with those of C_2^- and C_2^+, consistent with a regular bonding behavior in C_2. It is then shown that effective nuclear charge provides a logical basis for comparing the systems both in terms of D_0 and in terms of errors associated with various methods. Notably, all four tested density functionals fail in describing bonding in one of the two limits of effective nuclear charge, and meta functionals or any amount

of HF exchange does not change this very large error of 100 kJ/mol across the series, making this a prominent problem to density functional theory. The order of MO energies plays a critical role in understanding these challenges; it depends on the effective nuclear charge, because more diffuse $1\pi_u$ orbitals are less stabilized by higher nuclear charge than the σ orbitals. An analysis shows that the most difficult cases are CN and NO, which are the two open-shell systems.

ASSOCIATED CONTENT

Supporting Information

The supporting information is available free of charge on the ACS homepage. The file contains electronic energies at the aug-cc-pV5Z basis set level for molecules and atoms and ions (Table S1); errors in various methods vs. experimental D_0 (Table S2); computed zero point energies in a.u. and in kJ/mol (Table S3); basis set sensitivity study of N_2 (Table S4), O_2 (Table S5), NO (Table S6), CN (Table S7), CN^- (Table S8), NO^+ (Table S9), and CO (Table S10); scalar-relativistic corrections (Table S11); electronic energies of carbon species (Table S12); computed D_e of C_2, C_2^-, and C_2^+ (Table S13); basis set effects vs. bond strength (Figure S1); dependency of the HF electron density along the bond projection on basis set (Figure S2).

ACKNOWLEDGEMENTS

Computer time at the Aarhus supercomputer cluster ”Grendel” (formerly the Danish Center for Scientific Computing) is gratefully acknowledged.

REFERENCES

(1) Mulliken, R. S. Electronic population analysis on LCAO–MO molecular wave functions. I. *J. Chem. Phys.* **1955**, *23* (10), 1833–1840.

(2) Bader, R. F. W.; Bandrauk, A. D. Molecular charge distributions and chemical binding. III. The isoelectronic series N_2, CO, BF, and C_2, BeO, LiF. *J. Chem. Phys.* **1968**, *49* (4), 1653–1665.

(3) Lawson, D. B.; Harrison, J. F. Some observations on molecular orbital theory. *J. Chem. Educ* **2005**, *82* (8), 1205.

(4) Murad, F. Discovery of some of the biological effects of nitric oxide and its role in cell signaling (Nobel lecture). *Angew. Chemie Int. Ed.* **1999**, *38* (13-14), 1856–1868.

(5) Dawson, T. M.; Snyder, S. H. Gases as biological messengers: Nitric oxide and carbon monoxide in the brain. *J. Neurosci.* **1994**, *14* (9), 5147–5159.

(6) Bailey, D. C.; Langer, S. H. Immobilized transition-metal carbonyls and related catalysts. *Chem. Rev.* **1981**, *81* (2), 109–148.

(7) Harcourt, R. D. Transition metal complexes with CO, N_2, NO and O_2 ligands. In *Bonding in Electron-Rich Molecules*; Springer, 2016; pp 231–246.

(8) Frenking, G.; Fröhlich, N. The nature of the bonding in transition-metal compounds. *Chem. Rev.* **2000**, *100* (2), 717–774.

(9) Ford, P. C.; Lorkovic, I. M. Mechanistic aspects of the reactions of nitric oxide with transition-metal complexes. *Chem. Rev.* **2002**, *102* (4), 993–1018.

(10) Davidson, E. R. Electronic population analysis of molecular wavefunctions. *J. Chem. Phys.*

1967, *46* (9), 3320–3324.

(11) Gilmore, F. R. Potential energy curves for N_2, NO, O_2 and corresponding ions. *J. Quant. Spectrosc. Radiat. Transf.* **1965**, *5* (2), 369–389.

(12) Peterson, K. A.; Dunning, T. H. Intrinsic errors in several ab initio methods: The dissociation energy of N_2. *J. Phys. Chem.* **1995**, *99* (12), 3898–3901.

(13) Nesbet, R. K. Electronic structure of N_2, CO, and BF. *J. Chem. Phys.* **1964**, *40* (12), 3619–3633.

(14) Ruden, T. A.; Helgaker, T.; Jørgensen, P.; Olsen, J. Coupled-cluster connected quadruples and quintuples corrections to the harmonic vibrational frequencies and equilibrium bond distances of HF, N_2, F_2, and CO. *J. Chem. Phys.* **2004**, *121* (12), 5874–5884.

(15) Pietrzyk, P.; Zasada, F.; Piskorz, W.; Kotarba, A.; Sojka, Z. Computational spectroscopy and DFT investigations into nitrogen and oxygen bond breaking and bond making processes in model deNOx and deN_2O reactions. *Catal. Today* **2007**, *119* (1), 219–227.

(16) Siegbahn, P. E. M. OO bond cleavage and alkane hydroxylation in methane monooxygenase. *J. Biol. Inorg. Chem.* **2001**, *6* (1), 27–45.

(17) Shaik, S.; Chen, H. Lessons on O_2 and NO bonding to heme from ab initio multireference/multiconfiguration and DFT calculations. *J. Biol. Inorg. Chem.* **2011**, *16* (6), 841–855.

(18) Kepp, K. P. Heme: From quantum spin crossover to oxygen manager of life. *Coord. Chem. Rev.* **2017**, *344*, 363–374.

(19) Jensen, K. P.; Roos, B.; Ryde, U. O_2-binding to heme: Electronic structure and spectrum of oxyheme, studied by multiconfigurational methods. *J. Inorg. Biochem.* **2005**, *99*, 45–54.

(20) Jensen, K. P.; Roos, B. O.; Ryde, U. Erratum to "O_2-binding to heme: Electronic structure and spectrum of oxyheme, studied by multiconfigurational methods" [J. Inorg. Biochem. 99(1) (2004) 45–54]. *J. Inorg. Biochem.* **2005**, *99* (4), 978.

(21) Grunenberg, J. Quadruply bonded carbon. *Nat. Chem.* **2012**, *4* (3), 154–155.

(22) Grunenberg, J. Comment on "The nature of the fourth bond in the ground state of C_2: The quadruple bond conundrum." *Chem. Eur. J.* **2015**, *21* (47), 17126.

(23) Shaik, S.; Danovich, D.; Hiberty, P. C. Response to the comment by J. Grunenberg on "The nature of the fourth bond in the ground state of C_2: The quadruple bond conundrum"'. *Chem. Eur. J.* **2015**, *21* (47), 17127–17128.

(24) Danovich, D.; Hiberty, P. C.; Wu, W.; Rzepa, H. S.; Shaik, S. The nature of the fourth bond in the ground state of C_2: The quadruple bond conundrum. *Chem. Eur. J.* **2014**, *20* (21), 6220–6232.

(25) Hermann, M.; Frenking, G. The chemical bond in C_2. *Chem. Eur. J.* **2016**, *22* (12), 4100–4108.

(26) de Sousa, D. W. O.; Nascimento, M. A. C. Is there a quadruple bond in C_2? *J. Chem. Theory Comput.* **2016**, *12* (5), 2234–2241.

(27) Shaik, S.; Danovich, D.; Wu, W.; Su, P.; Rzepa, H. S.; Hiberty, P. C. Quadruple bonding in C_2 and analogous eight-valence electron species. *Nat. Chem.* **2012**, *4* (3), 195–200.

(28) Shaik, S.; Danovich, D.; Braida, B.; Hiberty, P. C. The quadruple bonding in C_2 reproduces the properties of the molecule. *Chem. Eur. J.* **2016**, *22* (12), 4116–4128.

(29) Piris, M.; Lopez, X.; Ugalde, J. M. The bond order of C_2 from a strictly N-representable natural orbital energy functional perspective. *Chem. Eur. J.* **2016**.

(30) Frenking, G.; Hermann, M. Critical comments on "One molecule, two atoms, three views, four bonds?" *Angew. Chemie* **2013**, *125* (23), 6036–6039.

(31) Zhong, R.; Zhang, M.; Xu, H.; Su, Z. Latent harmony in dicarbon between VB and MO theories through orthogonal hybridization of 3 sigma(g) and 2 sigma(u). *Chem. Sci.* **2016**, *7* (2), 1028–1032.

(32) West, A. C.; Schmidt, M. W.; Gordon, M. S.; Ruedenberg, K. Intrinsic resolution of molecular electronic wave functions and energies in terms of quasi-atoms and their interactions. *J. Phys. Chem. A* **2017**, *121* (5), 1086–1105.

(33) Ahlrichs, R.; Bär, M.; Häser, M.; Horn, H.; Kölmel, C. Electronic structure calculations on workstation computers: The program system Turbomole. *Chem. Phys. Lett.* **1989**, *162* (3), 165–169.

(34) Eichkorn, K.; Treutler, O.; Öhm, H.; Häser, M.; Ahlrichs, R. Auxiliary basis sets to approximate coulomb potentials. *Chem. Phys. Lett.* **1995**, *240* (4), 283–290.

(35) Weigend, F.; Häser, M. RI-MP2: First derivatives and global consistency. *Theor. Chem. Acc.* **1997**, *97* (1), 331–340.

(36) Tew, D. P.; Klopper, W.; Neiss, C.; Hättig, C. Quintuple-ζ quality coupled-cluster correlation energies with triple-ζ basis sets. *Phys. Chem. Chem. Phys.* **2007**, *9* (16), 1921–1930.

(37) Dunning, T. H. Gaussian basis sets for use in correlated molecular calculations. I. The atoms boron through neon and hydrogen. *J. Chem. Phys.* **1989**, *90* (2), 1007–1023.

(38) Polák, R.; Fišer, J. On the electronic structure of CN^-. *J. Mol. Struct. THEOCHEM* **2002**, *584* (1), 69–77.

(39) Weigend, F.; Ahlrichs, R. Balanced basis sets of split valence, triple zeta valence and quadruple zeta valence quality for H to Rn: Design and assessment of accuracy. *Phys. Chem. Chem. Phys.* **2005**, *7* (18), 3297–3305.

(40) Cowan, R. D.; Griffin, D. C. Approximate relativistic corrections to atomic radial wave functions. *J. Opt. Soc. Am.* **1976**, *66* (10), 1010–1014.

(41) Perdew, J. P.; Burke, K.; Ernzerhof, M. Generalized gradient approximation made simple. *Phys. Rev. Lett.* **1996**, *77* (18), 3865.

(42) Becke, A. D. Density-functional thermochemistry. III. The role of exact exchange. *J. Chem. Phys.* **1993**, *98* (7), 5648–5652.

(43) Stephens, P. J.; Devlin, F. J.; Chabalowski, C. F.; Frisch, M. J. Ab initio calculation of vibrational absorption and circular dichroism spectra using density functional force fields. *J. Phys. Chem.* **1994**, *98* (45), 11623–11627.

(44) Lee, C.; Yang, W.; Parr, R. G. Development of the Colle-Salvetti correlation-energy formula into a functional of the electron density. *Phys. Rev. B* **1988**, *37* (2), 785.

(45) Tao, J.; Perdew, J. P.; Staroverov, V. N.; Scuseria, G. E. Climbing the density functional ladder: Nonempirical meta generalized gradient approximation designed for molecules and solids. *Phys. Rev. Lett.* **2003**, *91* (14), 146401.

(46) Perdew, J. P.; Tao, J.; Staroverov, V. N.; Scuseria, G. E. Meta-generalized gradient approximation: Explanation of a realistic nonempirical density functional. *J. Chem. Phys.* **2004**, *120* (15).

(47) Klopper, W.; Helgaker, T. Extrapolation to the limit of a complete basis set for electronic structure calculations on the N_2 molecule. *Theor. Chem. Acc.* **1998**, *99* (4), 265–271.

(48) Halkier, A.; Helgaker, T.; Jørgensen, P.; Klopper, W.; Koch, H.; Olsen, J.; Wilson, A. K. Basis-set convergence in correlated calculations on Ne, N_2, and H_2O. *Chem. Phys. Lett.* **1998**, *286* (3), 243–252.

(49) Kong, L.; Bischoff, F. A.; Valeev, E. F. Explicitly correlated R12/F12 methods for electronic structure. *Chem. Rev.* **2011**, *112* (1), 75–107.

(50) Lee, T. J. Comparison of the T1 and D1 diagnostics for electronic structure theory: A new definition for the open-shell D1 diagnostic. *Chem. Phys. Lett.* **2003**, *372* (3), 362–367.

TOC Graphic

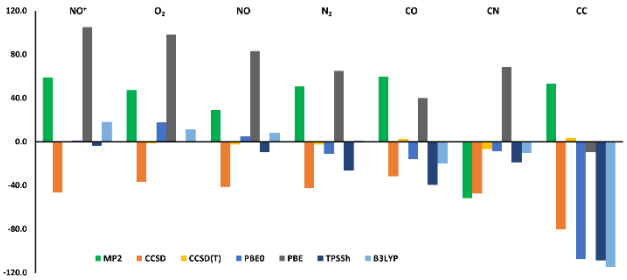
120.0
80.0
40.0
0.0
-40.0
-80.0
-120.0
NO+
O2
NO
N2
CO
CN
CC
MP2
CCSD
CCSD(T)
PBE0
PBE
TPSSh
B3LYP

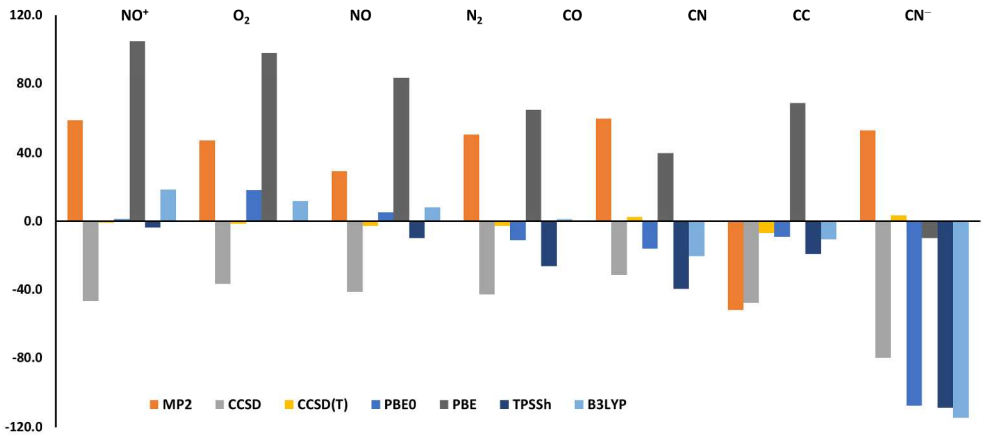

Figure 1

204x93mm (300 x 300 DPI)

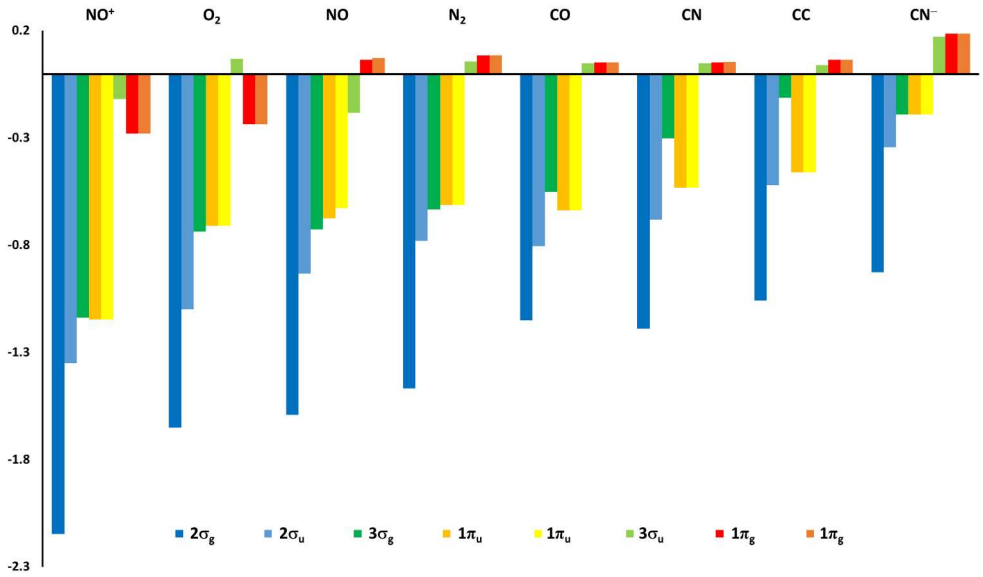

Figure 2

194x115mm (300 x 300 DPI)

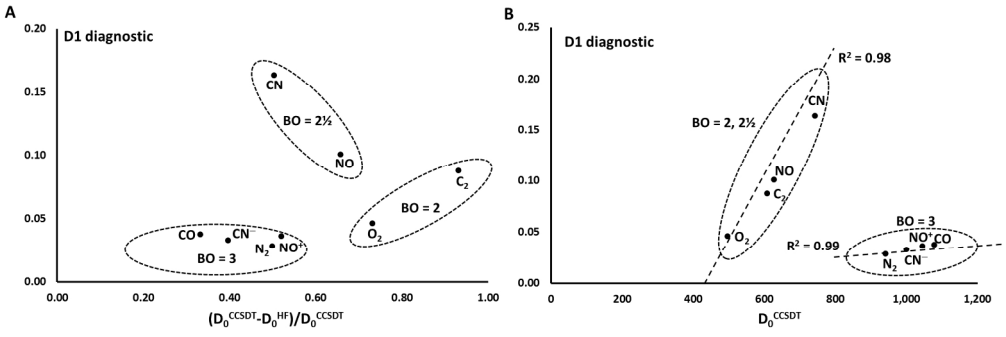

Figure 3

186x60mm (300 x 300 DPI)

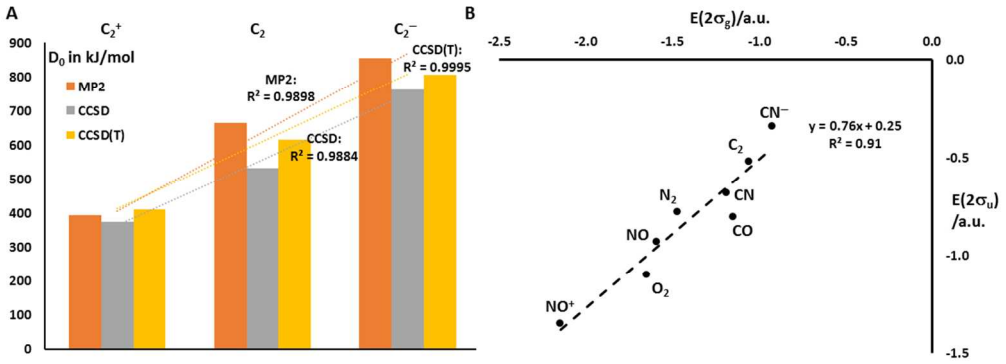

Figure 4

102x37mm (300 x 300 DPI)

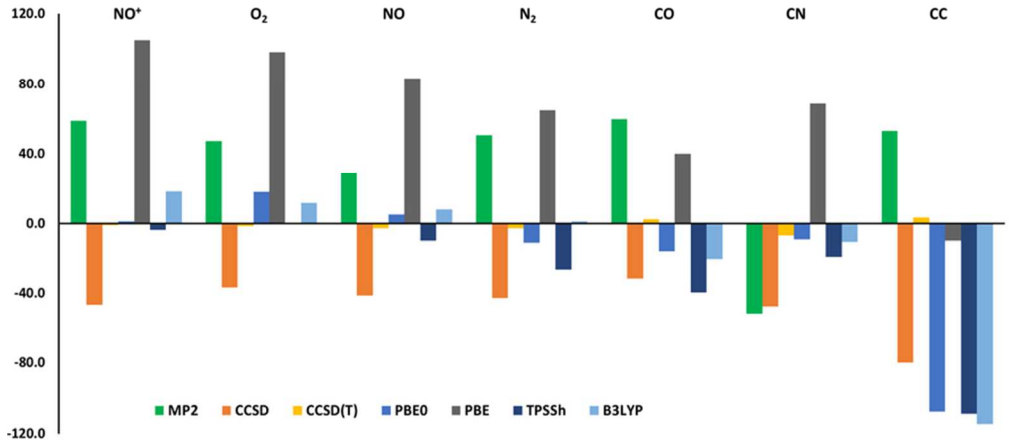

TOC graphic

37x17mm (600 x 600 DPI)